American Mineralogist, Volume 97, pages 1808–1811, 2012

LETTER

In situ observation of the breakdown of magnetite (Fe_3O_4) to Fe_4O_5 and hematite at high pressures and temperatures

ALAN B. WOODLAND,[1,*] DANIEL J. FROST,[2] DMYTRO M. TROTS,[2] KEVIN KLIMM,[1] AND MOHAMED MEZOUAR[3]

[1]Institut für Geowissenschaften, Universität Frankfurt, Altenhöferallee 1, 60438 Frankfurt, Germany
[2]Bayerisches Geoinstitut, Universität Bayreuth, 95440 Bayreuth, Germany
[3]ESRF, BP 220, 38027 Grenoble, France

ABSTRACT

In situ synchrotron X-ray powder diffraction measurements using a Paris-Edinburgh pressure cell were performed to investigate the nature of the high-pressure breakdown reaction of magnetite (Fe_3O_4). Refinement of diffraction patterns reveals that magnetite breaks down via a disproportionation reaction to Fe_4O_5 and hematite (Fe_2O_3) rather than undergoing an isochemical phase transition. This result, combined with literature data indicates (1) that this reaction occurs at ~9.5–11 GPa and 973–1673 K, and (2) these two phases should recombine at yet higher pressures to produce an *h*-Fe_3O_4 phase.

Keywords: Fe_4O_5, magnetite, phase transformation, high pressure

INTRODUCTION

Magnetite ($FeFe_2O_4$) is a mixed-valent phase that belongs to the spinel group of minerals. It is cubic (space group *Fd*3*m*) and possesses one tetrahedral and two octahedral sites per AB_2O_4 formula unit. Its phase relations are fundamental to the chemically simple Fe-O system, which forms the basis for understanding many more complex chemical systems relevant to the geological and material sciences. Considering that many other spinel-structured phases are known to undergo a phase transition at high pressures, the high-pressure stability of magnetite has also received much attention over the years (e.g., Mao et al. 1974; Huang and Bassett 1986; Pasternak et al. 1994; Fei et al. 1999; Lazor et al. 2004). At room-temperature magnetite undergoes an unquenchable transition at ~21 GPa to a phase often denoted as *h*-Fe_3O_4. The crystal structure of the *h*-Fe_3O_4 polymorph has been the subject of discussion for over 30 years. Mao et al. (1974) suggested it was monoclinic. In situ measurements at 823 K and 23.96 GPa in a diamond-anvil cell led Fei et al. (1999) to propose an orthorhombic $CaMn_2O_4$-type structure. More recent studies concluded that the related $CaTi_2O_4$-type structure was more consistent with the available diffraction data (Haavik et al. 2000; Dubrovinsky et al. 2003). In their in situ investigation at high pressures and temperatures, Schollenbruch et al. (2011) were able to determine that the phase boundary of magnetite–*h*-Fe_3O_4 transition was nearly isobaric (lying near 10 GPa) over a temperature range of 700–1400 °C. Unfortunately, the quality of their energy dispersive X-ray diffraction patterns did not permit the structure of *h*-Fe_3O_4 to be unambiguously determined. However, it was apparent that the new reflections that appeared in their diffraction patterns were inconsistent with both the $CaMn_2O_4$ and the $CaTi_2O_4$-type structures. This suggested an additional polymorph is stable at high pressures and temperatures, which they referred to as the "mystery phase." This phase had very similar *d*-spacings as those identified in an earlier study by Koch et al. (2004) on the Fe_3O_4-Fe_2SiO_4-Mg_2SiO_4 system.

We have undertaken a new in situ study at high pressure and temperature using angle dispersive X-ray powder diffraction in the hope of obtaining sufficient quality diffraction patterns to finally solve the crystal structure of *h*-Fe_3O_4 at the phase boundary with magnetite. For reasons that will become apparent, this was not a trivial exercise. However, with the recent report of a new Fe-oxide phase with Fe_4O_5 stoichiometry (Lavina et al. 2011), we are now able to unambiguously confirm that magnetite breaks down to a mixture of Fe_4O_5 and hematite at ~9.5–11 GPa and 973–1673 K, rather than transforming directly to a single isochemical polymorph.

EXPERIMENTAL METHODS

The magnetite starting material was the same as that used in the study of Schollenbruch et al. (2011), which was synthesized by reducing Fe_2O_3 at one atmosphere under conditions (1573 K and log f_{O_2} = –5.5) that should yield a stoichiometric composition (Dieckmann 1982). Stoichiometry was confirmed by the obtained unit-cell parameter of a_o = 8.3966(6) Å (Fleet 1984).

The experiments were performed using the on-line Paris-Edinburgh pressure cell on beamline ID27 at the European Synchrotron Radiation Facility (ESRF) in Grenoble, France. Recently installed sintered diamond anvils now permit pressures up to ~17 GPa to be reached at temperatures exceeding ~1300 K (Morard et al. 2007). An advantage of the Paris-Edinburgh cell over using a diamond-anvil cell is that clean diffraction patterns of the sample can be obtained with virtually no foreign reflections from either the anvils or the pressure medium. In addition, a new set of soller slits was recently installed before our experiments that significantly reduced beam divergence and improved the quality of the diffraction patterns by filtering out contributions from the materials in the pressure cell surrounding the sample (Morard et al. 2011).

Details of the experimental setup are reported in (Mezouar et al. 1999) and only briefly described here. The conical-shaped pressure cell was made of boron epoxy with an axial hole for the sample and a cylindrical graphite furnace. Magnetite powder was enclosed in a BN capsule. A 10:1 mixture of NaCl and Au was packed into a small hole bored into the side of the BN capsule. Diffraction patterns of this mixture permitted the pressure and temperature to be monitored during the

* E-mail: woodland@em.uni-frankfurt.de

0003-004X/12/0010–1808$05.00/DOI: http://dx.doi.org/10.2138/am.2012.4270

experiment by simultaneously fitting the cell parameters of these two phases to their corresponding equation of state (Crichton and Mezouar 2002). We used the equation of state for NaCl and Au from Brown (1999) and Jamieson et al. (1982), respectively. This meant that a thermocouple was unnecessary, allowing a sample volume large enough to obtain clean diffraction patterns from the sample material. The only drawback to this approach is that heating the sample is performed by increasing output power to the graphite resistance heater and that since resistance is pressure dependent, the temperature could not be changed independently of pressure and vice versa.

The diffraction patterns were measured using a fast, automated imaging-plate detector (Mezouar et al. 2005). The X-ray wavelength was determined by collecting and refining a diffraction pattern from a LaB_6 standard (λ = 0.37552 Å). The images were converted to 2Θ-intensity plots using Fit2d software (Hammersley 1997; Hammersley et al. 1996). The subsequent patterns were analyzed using either the GSAS software package (Larson and von Dreele 1988) and the EXPGUI interface of Toby (2001) or the FULLPROF software package (Rodriguez-Carvajal 1993).

The high-pressure breakdown of magnetite

Two experiments were performed following similar pressure-temperature paths; the paths for Mag_1 and Mag_2 are presented in Figure 1. Sample Mag_1 was compressed to ~12 GPa (i.e., beyond the stability field of magnetite, Schollenbruch et al. 2011) and then heated up to a temperature of about 1200 K. In a second experiment (Mag_2), the sample was brought to ~11 GPa and then heated progressively up to about 1200 K. In the latter experiment, the sample was subsequently depressurized to ~8.6 GPa while remaining at high temperature. In both experiments we were able to observe the appearance of a new set of reflections with the simultaneous disappearance of the magnetite reflections (Figs. 2A–2D). The large number of new reflections reveals that the new phase has a lower symmetry than the cubic-structured magnetite. However, apparent persistence of magnetite reflections in diffraction patterns obtained at *P-T* conditions well beyond the first appearance of the new phase presented difficulties in unambiguously identifying the set of reflections belonging to the new high-pressure phase. This hampered our ability to index the reflections and determine a crystal structure consistent with our data. Examination of individual diffraction patterns revealed that measurement Mag_2_057 obtained at 1366 K and 11.5 GPa was the best candidate for Rietveld analysis (Fig. 2D). The large number of reflections suggested a structure with a lower symmetry than orthorhombic; the symmetry associated with most reported *h*-Fe_3O_4 polymorphs (i.e., Fei et al. 1999; Haavik et al. 2000; Dubrovinsky et al. 2003). However, the monoclinic unit-cell suggested by Mao et al. (1974) was also quickly ruled out. Further attempts with different monoclinic structures began to yield some potential candidates, but there were always either reflections that remained unfit or the model structures possessed additional reflections with significant intensities that did not

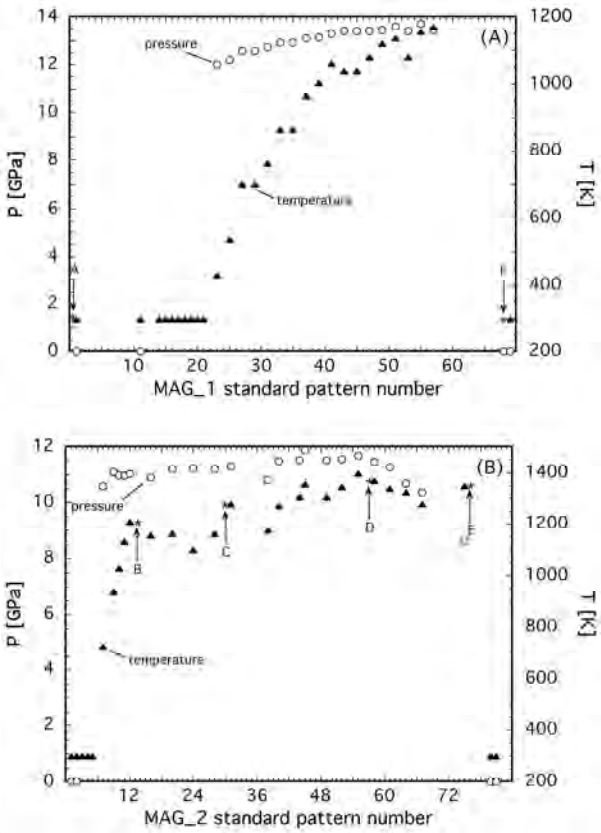

Figure 1. Pressure and temperature paths of experiments (**a**) Mag_1 and (**b**) Mag_2. "Standard pattern number" refers to the sequential diffraction pattern number of the experiment when the standard was measured to determine pressure and temperature (rather than when the sample was measured). Also shown are the positions (A–F) of the sample diffraction patterns presented in Figure 2.

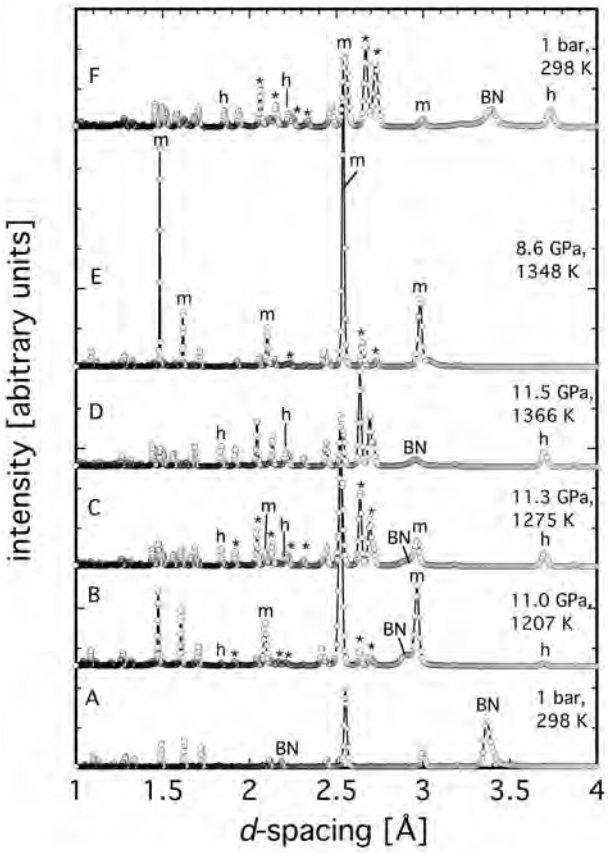

Figure 2. Selected integrated diffraction patterns obtained during experiments Mag_1 and Mag_2. BN = boron nitride, h = hematite, m = magnetite, * = Fe_4O_5. For clarity only selected peaks are labeled. Patterns **A**–**F** refer to the (*P-T*) points on the trajectory in Figure 1. Note the high quality of the patterns.

appear in the diffraction pattern.

The recent report of a new high-pressure Fe-oxide phase with Fe_4O_5 stoichiometry (Lavina et al. 2011) posed the tantalising possibility that Fe_3O_4 might in fact break down to more than one phase, thus explaining the large number of reflections in our diffraction patterns. This would imply the following type of disproportionation reaction that yields hematite along with Fe_4O_5:

$$\underset{\text{mt}}{2\,Fe_3O_4} = \underset{\text{new phase}}{Fe_4O_5} + \underset{\text{hem}}{Fe_2O_3} \quad (1)$$

Using structural data for the orthorhombic $CaFe_3O_5$-type Fe_4O_5 phase from Lavina et al. (2011), a Rietveld refinement of diffraction pattern Mag_2_057 gave an excellent fit including a large number of small reflections at small *d*-spacings (Fig. 3). Details of the refinement are provided in a supplementary CIF[1]. The resulting unit-cell parameters of the Fe_4O_5 phase and hematite at 1366 K and 11.5 GPa are given in Table 1, along with the derived reliability factors of the refinement. Subsequent refinements of other diffraction patterns collected during both experiments were consistent with either the assemblage Fe_4O_5 + hematite or with a mixture of these two phases along with magnetite. Refinement of the molar proportions of the products consistently yielded a ratio of 2/3 Fe_4O_5 to 1/3 hematite, which are the relative proportions expected from reaction 1 (i.e., 4/6 of the available Fe in Fe_4O_5 and 2/6 of the Fe in Fe_2O_3). These relative proportions were observed even in patterns containing coexisting magnetite. Thus our experiments give direct evidence for magnetite breaking down at ~900 K and ~10–13 GPa following reaction 1.

Reassessment of a number of energy-dispersive diffraction patterns from the study of Schollenbruch et al. (2011) revealed the assemblage Fe_4O_5 + hematite ± magnetite to be consistent with the observed reflections, even if reliable refinement of these patterns was not possible. This re-analysis indicates that reaction 1 describes the breakdown of magnetite over a wide temperature range from 973 to 1673 K at a pressure of ~9.5–11 GPa.

The reformation of magnetite and ΔV of reaction

Toward the end of experiment Mag_2 the pressure was slowly released while maintaining a high temperature at ~1350 K, providing the opportunity to observe the formation of magnetite at the expense of Fe_4O_5 + hematite. The diffraction rings in the images corresponding to the newly formed magnetite were spotty, indicating coarsening through rapid grain growth. This led to abnormal peak intensities in the integrated diffraction patterns (see Fig. 2E), making it difficult to assess the mechanism of magnetite formation from our experimental results.

On the other hand, experiment Mag_1 was more rapidly brought down to room temperature and subsequently decompressed. A diffraction pattern taken at ambient conditions revealed that a significant amount of Fe_4O_5 and hematite was still present, along with magnetite (Fig. 2F). Rietveld analysis of this diffraction pattern yielded molar volumes for of 53.79(1) cm^3 for Fe_4O_5, 30.40(1) cm^3 for hematite and 44.58(1) cm^3 for the coexisiting magnetite. This value for Fe_4O_5 agrees very well with that reported by Lavina et al. (2011) and the value for magnetite is in perfect agreement with that reported by Woodland and Angel (2000). This results in a $\Delta V° = -4.97(2)$ cm^3 for reaction 1 at ambient conditions, consistent with Fe_4O_5 + hematite being the high-pressure assemblage. Similar analysis of diffraction pattern Mag_2_030 (Fig. 2C), which was measured at 1275 K and 11.3 GPa (near the reaction boundary as determined by Schollenbruch et al. 2011) yielded a $\Delta V° = -4.76(2)$ cm^3. Thus although some variation in ΔV due to differing compressibility and thermal expansion for the three phases is expected, this variation is minor.

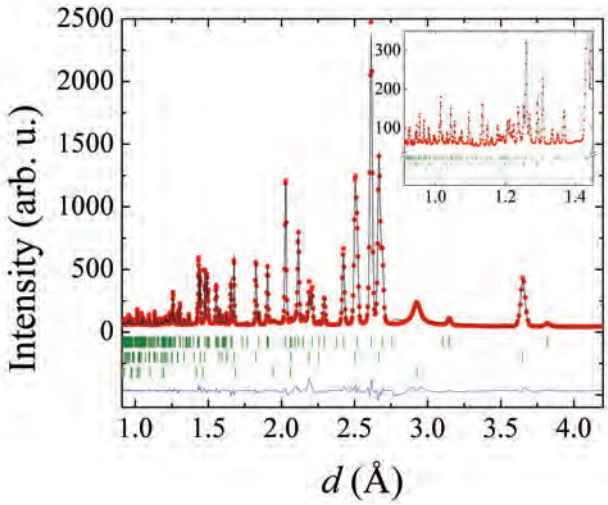

Figure 3. Results of Rietveld refinement of diffraction pattern Mag_2_057 (Fig. 2D) over the measured range of *d*-spacings from 4.1 to 0.9 Å. A close-up of the *d*-spacing range 1.45 to 0.9 Å. Notice how well the many reflections with small *d*-spacings are fit using the assemblage of Fe_4O_5 + hematite. (Color online.)

Table 1. Results of the refinement of pattern Mag_2_057 with Fe_4O_5 and Fe_2O_3 using the FULLPROF software package

Wavelength (Å)	0.37552
d-spacing of NaCl(200)* (Å)	2.629(1)
d-spacing of Au(111)* (Å)	2.338(1)
Pressure† (GPa)	11.5(2)
Temperature† (K)	1366(50)
Lattice parameters for Fe_4O_5 (Å)	a = 2.87366(8), b = 9.6940(3), c = 12.4116(4)
Volume of Fe_4O_5 ($Å^3$)	345.753(18)
Lattice parameters for Fe_2O_3 (Å)	a = 5.00846(13), c = 13.5315(4)
Volume of Fe_2O_3 ($Å^3$)	293.958(14)
Rp	4.66
Rwp	7.43

Notes: Fe_4O_5 was refined in the orthorhombic space group *Cmcm*. Unit-cell parameters and volumes of product phases (Fe_4O_5 and Fe_2O_3) from diffraction pattern Mag_2_057.
* Measured in pattern Mag_2_058 directly after the sample measurement.
† Calculated using combination of equations of state for NaCl and Au from Brown (1999) and Jamieson et al. (1982), respectively.

Concluding remarks

Like other studies on magnetite, the high-pressure assemblage was not recoverable after quenching and decompression. On the

[1] Deposit item AM-12-098, CIF. Deposit items are available two ways: For a paper copy contact the Business Office of the Mineralogical Society of America (see inside front cover of recent issue) for price information. For an electronic copy visit the MSA web site at http://www.minsocam.org, go to the *American Mineralogist* Contents, find the table of contents for the specific volume/issue wanted, and then click on the deposit link there.

other hand, Lavina et al. (2011) were able to recover Fe_4O_5 from their experiments and perform a structural refinement at ambient conditions. Thus it would appear that it is the assemblage of Fe_4O_5 + hematite that is generally unquenchable, meaning that the presence of hematite destabilizes the Fe_4O_5 phase. In bulk compositions with lower $Fe^{3+}/\Sigma Fe$ where hematite is not present, Fe_4O_5 can remain stable until conditions are reached where it breaks down to the low-pressure assemblage of magnetite + wüstite. The low-pressure stability limit of Fe_4O_5 apparently lies between 5 and 10 GPa (Lavina et al. 2011). However, going by the first appearance of the "mystery" phase in the experiments of Koch et al. (2004), the stability limit would lie at ~9 GPa, which is not much different from the breakdown reaction of magnetite as documented by Schollenbruch et al. (2011). An in-depth reanalysis of their data in light of the stability of the Fe_4O_5 phase will be the subject of a future communication.

Combining our results with the observations of Schollenbruch et al. (2011), Fei et al. (1999), Haavik et al. (2000), and Dubrovinsky et al. (2003), it is apparent that the assemblage Fe_4O_5 + hematite remains stable up to ~16 GPa at 1573 K, but must recombine to form a new phase with Fe_3O_4 stoichiometry (i.e., *h*-Fe_3O_4) at yet higher pressures. Considering that the measurements reported by the later three authors were made under differing *P-T* conditions it is conceivable that stability fields for several *h*-Fe_3O_4 phases could exist, similar to that reported for $FeCr_2O_4$ (Chen et al. 2003). Thus the phase diagram for Fe_3O_4 at high pressures (and temperatures) must be significantly more complex than previously thought.

Acknowledgments

The initial part of this study was supported by grants from the Deutsche Forschungsgemeinschaft within the aegis of the priority program 1236 (Wo 652/9-1, FR 1555/4). We recognize ERC advanced grant no. 227893 "DEEP" funded through the EU 7th Framework Programme. The comments of three anonymous reviewers and the associate editor helped to improve the manuscript.

References cited

Brown, J.M. (1999) The NaCl pressure standard. Journal of Applied Physics, 86, 5801–5808.

Chen, M., Shu, J., Mao, H.-K., Xie, X., and Hemley, R.J. (2003) Natural occurrence and synthesis of two new postspinel polymorphs of chromite. Proceedings of the National Academy of Sciences (PNAS), 100, 14651–14654.

Crichton, W.A. and Mezouar, M. (2002) Noninvasive pressure and temperature estimation in large-volume apparatus by equation-of-state cross-calibration. High Temperatures-High Pressures, 34, 235–242.

Dieckmann, R. (1982) Defects and cation diffusion in magnetite (IV)-nonstoichiometry and point-defect structure of magnetite $Fe_{3-\delta}O_4$. Berichte der Bunsen-Gesellschaft-Physical Chemistry Chemical Physics, 86, 112–118.

Dubrovinsky, L.S., Dubrovinskaia, N.A., McCammon, C., Rozenberg, G.K., Ahuja, R., Osorio-Guillen, J.M., Dmitriev, V., Weber, H.P., Le Bihan, T., and Johansson, B. (2003) The structure of the metallic high-pressure Fe_3O_4 polymorph: experimental and theoretical study. Journal of Physics-Condensed Matter, 15, 7697–7706.

Fei, Y.W., Frost, D.J., Mao, H.K., Prewitt, C.T., and Häusermann, D. (1999) In situ structure determination of the high-pressure phase of Fe_3O_4. American Mineralogist, 84, 203–206.

Fleet, M.E. (1984) The structure of magnetite: Two annealed natural magneites, $Fe_{3.005}O_4$ and $Fe_{2.96}Mg_{0.04}O_4$. Acta Crystallography, C40, 1491–1493.

Haavik, C., Stølen, S., Fjellvåg, H., Hanfland, M., and Häusermann, D. (2000) Equation of state of magnetite and its high-pressure modification: Thermodynamics of the Fe-O system at high pressure. American Mineralogist, 85, 514–523.

Hammersley, A.P. (1997) FIT2D: An introduction and overview. ESRF Internal Rep. ESRF97HA02T, European Synchrotron Radiation Facility, Grenoble, France.

Hammersley, A.P., Svensson, S.O., Hanfland, M., Fitch, A.N., and Häusermann, D. (1996) Two-Dimensional Detector Software: From Real Detector to Idealised Image or Two-Theta Scan. High Pressure Research, 14, 235–248.

Huang, E. and Bassett, W.A. (1986) Rapid-determination of Fe_3O_4 phase-diagram by synchrotron radiation. Journal of Geophysical Research, 91(B5), 4697–4703.

Jamieson, J., Fritz, J., and Manghnani, M. (1982) Pressure measurement at high temperature in X-ray diffraction studies: Gold as a primary standard. In S. Akimoto and M. Manghnani, Eds., High Pressure Research in Geophysics, p. 27–48. Center for Academic Publishing of Japan, Tokyo.

Koch, M., Woodland, A.B., and Angel, R.J. (2004) Stability of spinelloid phases in the system Fe_3O_4–Fe_2SiO_4–Mg_2SiO_4 at 1100°C and up to 10.5 GPa. Physics of the Earth and Planetary Interiors, 143–144, 171–183.

Larson, A.C. and von Dreele, R.B. (1988) General Structure Analysis System (GSAS). Los Alamos National Laboratory Report LAUR 86-748.

Lavina, B., Dera, P., Kim, E., Meng, Y., Downs, R.T., Weck, P.F., Sutton, S.R., and Zhao, Y. (2011) Discovery of the recoverable high-pressure iron oxide Fe_4O_5. Proceedings of the National Academy of Sciences (PNAS), 108, 17281–17285.

Lazor, P., Shebanova, O.N., and Annersten, H. (2004) High-pressure study of stability of magnetite by thermodynamic analysis and synchrotron X-ray diffraction. Journal of Geophysical Research, 109, B05201.

Mao, H.K., Takahash, T., Bassett, W.A., Kinsland, G.L., and Merrill, L. (1974) Isothermal compression of magnetite to 320 Kbar and pressure-induced phase-transformation. Journal of Geophysical Research, 79, 1165–1170.

Mezouar, M., Crichton, W.A., Bauchau, S., Thurel, F., Witsch, H., Torrecillas, F., Blattmann, G., Marion, P., Dabin, Y., Chavanne, J., and others. (2005) Development of a new state-of-the-art beamline optimized for monochromatic single-crystal and powder X-ray diffraction under extreme conditions at the ESRF. Journal of Synchrotron Radiation, 12, 659–664.

Mezouar, M., Le Bihan, T., Libotte, H., Le Godec, Y., and Häusermann, D. (1999) Paris-Edinburgh large-volume cell coupled with a fast imaging-plate system for structural investigation at high pressure and high temperature. Journal of Synchrotron Radiation, 6, 1115–1119.

Morard, G., Mezouar, M., Bauchau, S., Alvarez-Murga, M., Hodeau, J.L., and Garbarino, G. (2011) High efficiency multichannel collimator for structural studies of liquids and low-Z materials at high pressures and temperatures. Review of Scientific Instruments, 82, 023904.

Morard, G., Mezouar, M., Rey, N., Poloni, R., Merlen, A., Le Floch, S., Toulemonde, P., Pascarelli, S., San-Miguel, A., Sanloup, C., and Fiquet, G. (2007) Optimization of Paris-Edinburgh press cell assemblies for in situ monochromatic X-ray diffraction and X-ray absorption. High Pressure Research, 27, 223–233.

Pasternak, M.P., Nasu, S., Wada, K., and Endo, S. (1994) High-pressure phase of magnetite. Physical Review B, 50, 6446–6449.

Rodriguez-Carvajal, J. (1993) Recent advances in magnetic structure determination by neutron powder diffraction. Physica B, 192, 55–69.

Schollenbruch, K., Woodland, A. B., Frost, D. J., Wang, Y., Sanehira, T., and Langenhorst, F. (2011) In situ determination of the spinel – post-spinel transition in Fe_3O_4 at high temperature and pressure by synchrotron X-ray diffraction. American Mineralogist, 96, 820–827, DOI: 10.2138/am.2011.3642.

Toby, B.H. (2001) EXPGUI, a graphical user interface for GSAS. Journal of Applied Crystallography, 34, 210–213.

Woodland, A.B. and Angel, R.J. (2000) Phase relations in the system fayalite-magnetite at high pressures and temperatures. Contributions to Mineralogy and Petrology, 139, 734–747.

Manuscript received June 20, 2012
Manuscript accepted July 17, 2012
Manuscript handled by Ian Swainson

```
#######################################################
#######################
###      FullProf-generated CIF output file  (version:
February 2008)      ###
###      Template of CIF submission form for structure
report              ###
#######################################################
#######################

# This file has been generated using FullProf.2k taking
one example of
# structure report provided by Acta Cryst. It is given
as a 'template' with
# filled structural items. Many other items are left
unfilled and it is the
# responsibility of the user to properly fill or
suppress them. In principle
# all question marks '?' should be replaced by the
appropriate text or
# numerical value depending on the kind of CIF item.
# See the document: cif_core.dic (URL:
http://www.iucr.org) for details.

# Please notify any error or suggestion to:
#           Juan Rodriguez-Carvajal (jrc@ill.eu)
# Improvements will be progressively added as needed.

#=======================================================
=======================
 data_global
#=======================================================
=======================



#=======================================================
=======================

# 1. SUBMISSION DETAILS

_publ_contact_author_name            'Alan Woodland,
cif by D.M.Trots'  #
_publ_contact_author_address            # Address of
author for correspondence
; 'Institut fuer Geowissenschaften, Uni Frankfurt,
```

```
60438 Frankfurt'
;
_publ_contact_author_email           'woodland@em.uni-
frankfurt.de'
_publ_contact_author_fax             '++49 (0)69 798-
40121'
_publ_contact_author_phone           '++49 (0)69 798-
40119'


_publ_requested_journal              'Submitted to
American Mineralogist'




# 3. TITLE AND AUTHOR LIST

_publ_section_title
; 'In situ observation of the breakdown of Fe3O4 to
Fe4O5 and Fe2O3 at HP/HT'
;

# The loop structure below should contain the names and
addresses of all
# authors, in the required order of publication. Repeat
as necessary.

loop_
    _publ_author_name
    _publ_author_footnote
    _publ_author_address
' A. Woodland et al.'    #<--'Last name, first name'
;
;
;
;

#=================================================================
========================

# 4. TEXT

_publ_section_synopsis
;  ?
```

```
;
_publ_section_abstract
; ?
;
_publ_section_comment
; ?
;
_publ_section_exptl_prep      # Details of the
preparation of the sample(s)
                              # should be given here.
; ?
;
_publ_section_exptl_refinement
; ?
;
_publ_section_references
; ?
;
_publ_section_figure_captions
; ?
;
_publ_section_acknowledgements
; ?
;

#=========================================================
========================

#=========================================================
========================
# If more than one structure is reported, the remaining
sections should be
# completed per structure. For each data set, replace
the '?' in the
# data_? line below by a unique identifier.

data_Fe4O5

#=========================================================
========================

# 5. CHEMICAL DATA

_chemical_name_systematic
; ?
```

```
;
_chemical_name_common              'Fe4O5'
_chemical_formula_moiety           ?
_chemical_formula_structural       'Fe16O20'
_chemical_formula_analytical       'Fe4O5'
_chemical_formula_iupac            Fe4O5
_chemical_formula_sum              'Fe4 O5'
_chemical_formula_weight           303.388
_chemical_melting_point            ?
_chemical_compound_source          'Multianvil in-situ
experiment'
_exptl_crystal_density_diffrn        5.82
                                          # natural
products

loop_
    _atom_type_symbol
    _atom_type_scat_Cromer_Mann_a1
    _atom_type_scat_Cromer_Mann_b1
    _atom_type_scat_Cromer_Mann_a2
    _atom_type_scat_Cromer_Mann_b2
    _atom_type_scat_Cromer_Mann_a3
    _atom_type_scat_Cromer_Mann_b3
    _atom_type_scat_Cromer_Mann_a4
    _atom_type_scat_Cromer_Mann_b4
    _atom_type_scat_Cromer_Mann_c
    _atom_type_scat_dispersion_real
    _atom_type_scat_dispersion_imag
    _atom_type_scat_source
fe    11.76950   4.76110   7.35730   0.30720   3.52220
15.35350
       2.30450  76.88050   1.03690   0.24400   0.54500

International_Tables_for_Crystallography_Vol.C(1991)_Ta
bles_6.1.1.4_and_6.1.1.5
o      3.04850  13.27710   2.28680   5.70110   1.54630
0.32390
       0.86700  32.90890   0.25080   0.00300   0.00400

International_Tables_for_Crystallography_Vol.C(1991)_Ta
bles_6.1.1.4_and_6.1.1.5

#=========================================================
=======================
```

```
# 6. POWDER SPECIMEN AND CRYSTAL DATA

_symmetry_cell_setting                Orthorhombic
_symmetry_space_group_name_H-M       'C m c m'
_symmetry_space_group_name_Hall      '-C 2c 2'

loop_
    _symmetry_equiv_pos_as_xyz   #<--must include
'x,y,z'
'x,y,z'
'x,-y,-z'
'-x,y,-z+1/2'
'-x,-y,z+1/2'
'-x,-y,-z'
'-x,y,z'
'x,-y,z+1/2'
'x,y,-z+1/2'
'x+1/2,y+1/2,z'
'x+1/2,-y+1/2,-z'
'-x+1/2,y+1/2,-z+1/2'
'-x+1/2,-y+1/2,z+1/2'
'-x+1/2,-y+1/2,-z'
'-x+1/2,y+1/2,z'
'x+1/2,-y+1/2,z+1/2'
'x+1/2,y+1/2,-z+1/2'

_cell_length_a                        2.87366(8)
_cell_length_b                        9.6940(3)
_cell_length_c                        12.4116(4)
_cell_angle_alpha                     90.00000
_cell_angle_beta                      90.00000
_cell_angle_gamma                     90.00000
_cell_volume                          345.751(18)
_cell_formula_units_Z                 4
_cell_measurement_temperature         ?
_cell_special_details
; ?
;
_pd_char_colour                    'black'

#=========================================================
========================

# 7. EXPERIMENTAL DATA
```

```
# The following item is used to identify the equipment
used to record
# the powder pattern when the diffractogram was
measured at a laboratory
# other than the authors' home institution, e.g. when
neutron or synchrotron
# radiation is used.



_diffrn_radiation_wavelength     0.375518
_diffrn_source                   'ID27 at ESRF'
_diffrn_radiation_type           synchrotron
_diffrn_measurement_device_type      'Paris-Edinburgh
pressure cell '


#  The following four items give details of the
measured (not processed)
#  powder pattern.  Angles are in degrees.

_pd_meas_number_of_points         1455
_pd_meas_2theta_range_min         5.00141
_pd_meas_2theta_range_max         25.28605
_pd_meas_2theta_range_inc         0.013961

#=====================================================
=======================

# 8. REFINEMENT DATA


#  The following profile R-factors are NOT CORRECTED
for background
#  The sum is extended to all non-excluded points.
#  These are the current CIF standard

_pd_proc_ls_prof_R_factor                4.6645
_pd_proc_ls_prof_wR_factor               7.4262
_pd_proc_ls_prof_wR_expected             8.9672
_refine_ls_goodness_of_fit_all           0.69



#  Items related to LS refinement
```

```
_refine_ls_R_I_factor                    3.7738
_refine_ls_number_reflns                     204
_refine_ls_number_parameters                  32
_refine_ls_number_restraints                   0

# The following four items apply to angular dispersive
measurements.
# 2theta minimum, maximum and increment (in degrees)
are for the
# intensities used in the refinement.

_pd_proc_2theta_range_min                  5.0014
_pd_proc_2theta_range_max                 25.2860
_pd_proc_2theta_range_inc                0.013961
_pd_proc_wavelength                      0.375518



# The following items are used to identify the programs
used.


_computing_structure_refinement      FULLPROF


#=====================================================
=======================

# 9. ATOMIC COORDINATES AND DISPLACEMENT PARAMETERS

loop_
    _atom_site_label
    _atom_site_fract_x
    _atom_site_fract_y
    _atom_site_fract_z
    _atom_site_U_iso_or_equiv
    _atom_site_occupancy
    _atom_site_adp_type              # Not in version
2.0.1
    _atom_site_type_symbol
 Fe1   0.00000     0.00000     0.00000     0.030(2)
1.00000    Uiso Fe
 Fe2   0.00000     0.2619(5)   0.1176(3)   0.0317(11)
```

```
1.00000    Uiso Fe
 Fe3   0.00000     0.5079(6)   0.25000     0.040(2)
1.00000    Uiso Fe
 O1   0.00000     0.165(2)    0.25000     0.019(6)
1.00000    Uiso O
 O2   0.00000     0.3577(15)  0.5485(14)  0.036(5)
1.00000    Uiso O
 O3   0.00000     0.0937(17)  0.6448(11)  0.026(4)
1.00000    Uiso O

# Note: if the displacement parameters were refined
anisotropically
# the U matrices should be given as for single-crystal
studies.

#=========================================================
========================

# 10. DISTANCES AND ANGLES / MOLECULAR GEOMETRY

_geom_special_details                ?

loop_
    _geom_bond_atom_site_label_1
    _geom_bond_atom_site_label_2
    _geom_bond_site_symmetry_1
    _geom_bond_site_symmetry_2
    _geom_bond_distance
    _geom_bond_publ_flag

Fe1 Fe2 . . 2.9281(54) ?


loop_
_geom_angle_atom_site_label_1
_geom_angle_atom_site_label_2
_geom_angle_atom_site_label_3
_geom_angle_site_symmetry_1
_geom_angle_site_symmetry_2
_geom_angle_site_symmetry_3
_geom_angle
_geom_angle_publ_flag
Fe1   O3   O3   .   .   .   180   ?
```